



Universal signatures of the metamagnetic quantum critical endpoint: Application to CeRu₂Si₂

Franziska Weickert, Manuel Brando, and Frank Steglich

Max-Planck-Institut für Chemische Physik fester Stoffe, 01187 Dresden, Germany

Philipp Gegenwart

I. Physikalisches Institut, Georg-August-Universität Göttingen, 37077 Göttingen, Germany

Markus Garst

Institut für Theoretische Physik, Universität zu Köln, 50938 Köln, Germany

and Physik Department, Technische Universität München, 85748 Garching, Germany.

(Received 9 February 2010; published 30 April 2010)

A quantum critical endpoint related to a metamagnetic transition causes distinct signatures in the thermodynamic quantities of a compound. We argue that, irrespective of the microscopic details of the considered material, the diverging differential susceptibility combined with the Ising symmetry of the endpoint give rise to a number of characteristic metamagnetic phenomena. In the presence of a magnetoelastic coupling, one finds a correspondence of susceptibility, magnetostriction, and compressibility and, as a result, a pronounced crystal softening, a diverging Grüneisen parameter, a sign change of thermal expansion $\alpha(H)$, and a minimum in the specific-heat coefficient $\gamma(H)$. We illustrate these signatures and their relation on the metamagnetic crossover at 8 T in the prototypical heavy-fermion system CeRu₂Si₂.

DOI: [10.1103/PhysRevB.81.134438](https://doi.org/10.1103/PhysRevB.81.134438)

PACS number(s): 75.30.Kz, 71.27.+a

I. INTRODUCTION

Emergent universality close to critical points is one of the most fascinating phenomena in physics. Materials with utterly distinct microscopic composition might exhibit similar behavior close to a second-order phase transition if they only belong to the same universality class. Universality is also expected close to a critical endpoint that terminates a line of first-order transitions such as, for example, in the phase diagram of the liquid-gas transition. Such an endpoint is characterized by Ising universality, though the Ising order parameter is sometimes not simply related to measurable quantities.

Another example of an Ising critical endpoint can be found in metamagnetic materials. Metamagnetism is often casually described as a superlinear rise of the magnetization $M(H)$ at some finite critical field H_m . With decreasing temperature, such a smooth metamagnetic crossover might evolve into a sharp first-order jump of $M(H)$ identifying an endpoint (T_{ep}, H_m) in the phase diagram plane defined by temperature, T , and magnetic field H .^{1,2} In the context of the metamagnetic material Sr₃Ru₂O₇ it was pointed out^{3,4} that an interesting situation arises if the endpoint temperature T_{ep} can be tuned toward zero, $T_{\text{ep}} \rightarrow 0$, by a certain external control parameter resulting in a quantum critical endpoint (QCEP) for $T_{\text{ep}}=0$. Such an Ising QCEP differs from its classical counterpart at finite T_{ep} because the dynamics of the Ising order parameter has to be taken into account explicitly in the quantum case.⁴ This dynamics then generate the temperature dependence in its vicinity giving rise to quantum critical scaling. For example, the differential susceptibility at H_m diverges by definition with decreasing temperature with a characteristic powerlaw, $\chi \sim T^{-x}$. Despite the fact that a QCEP can be hardly realized in any material due to the required fine-tuning $T_{\text{ep}}=0$, it might nevertheless control ther-

modynamics in an extended temperature and field range if it is only close in parameter space. This motivates us to look for universal signatures of the metamagnetic QCEP in various metamagnetic compounds.

In the present work, we concentrate on the canonical heavy-fermion material CeRu₂Si₂, which crystallizes in the tetragonal ThCr₂Si₂ structure and shows a pronounced metamagnetic crossover for field parallel to the crystallographic c direction with a steep rise in the magnetization $M(H)$ at $\mu_0 H_m \approx 8$ T.⁵ Over the last 20 years, its properties close to the critical field H_m have been intensively investigated by various experimental methods promoting it to be one of the best-studied metamagnetic metals, cf. the review Ref. 6. It has been noted early on that the metamagnetic signatures are mirrored by strong anomalies in dilatometry due to magnetoelastic coupling.⁷ Close to H_m one observes a remarkable large Grüneisen parameter,⁸ a sign change of the thermal expansion,⁹ and a strong crystal softening.¹⁰ Moreover, the specific-heat coefficient $\gamma(H)$ shows a characteristic double peak structure close to the critical field H_m .¹¹ Although the temperature dependence of thermodynamics is anomalous, Fermi-liquid behavior is recovered at lowest temperatures for all magnetic fields. In particular, the differential susceptibility at H_m first increases with decreasing T but then starts to saturate at a temperature on the order of $T^*=0.5$ K.^{12,13} In the past, the experimental results have been often interpreted within a scaling ansatz for the entropy of the form $S[H/H_m(p), T/T_0(p)]$, with the magnetic field H , temperature T , pressure-dependent critical field $H_m(p)$, and the temperature scale $T_0(p)$.^{8,14–16} This phenomenological approach was quite successful to account for the observed relations between the H dependence of various thermodynamic quantities in the low-temperature limit. However, it did not provide an explanation for the huge anomalies themselves such as, for example, the large Grüneisen parameter. Since then, a

number of microscopic theories based on the periodic Anderson or Hubbard model have been put forward for metamagnetism in heavy-fermion materials^{17–20} that qualitatively explained many of the observed features in CeRu₂Si₂.

Nevertheless, in a previous comparison²¹ of CeRu₂Si₂ with the ruthenate Sr₃Ru₂O₇ it was already noted that both compounds share similar metamagnetic anomalies despite their microscopic differences. This encourages us to speculate that some of these anomalies are not specific to the microscopics of CeRu₂Si₂ but are, in fact, associated with the emergent universality expected close to a metamagnetic QCEP. Note that the importance of critical magnetic fluctuations in this material has been anticipated early on.^{9,14} In the following, we demonstrate that, actually, some of the most striking metamagnetic features in CeRu₂Si₂ can be naturally explained within a QCEP scenario. We argue that the emergent Ising symmetry combined with the enhanced differential susceptibility give rise to the following generic phenomena close to a metamagnetic QCEP: (1) a correspondence between susceptibility, magnetostriction and elastic constants, and, as a consequence, (2) a pronounced crystal softening, (3) an enhanced Grüneisen parameter, (4) a sign change of the thermal expansion, and (5) a minimum of the specific heat coefficient, $\gamma(H)$, with two accompanying side peaks. Note, however, that the QCEP itself is not realized, neither in Sr₃Ru₂O₇ nor in CeRu₂Si₂. Whereas in the ruthenate it is masked by a thermodynamic phase,²² the saturation of the differential susceptibility in CeRu₂Si₂ and the concomitant onset of Fermi-liquid behavior indicates that the QCEP is close but still off in parameter space, its distance measured by the saturation temperature T^* . For this reason the sharp increase in the magnetization in CeRu₂Si₂ is mostly called *metamagnetic-like* transition or *metamagnetic crossover* in the literature.⁵ It is an open question whether there exists any tuning parameter that lowers the saturation temperature T^* further to bring CeRu₂Si₂ closer to quantum criticality. Attempts to tune the system to the QCEP or even to a first-order phase transition by applying pressure²³ or Ge doping on the Si site,²⁴ the latter being equivalent to negative pressure, failed. In both cases the thermodynamic signatures at the metamagnetic crossover are even broader compared to the pure system at ambient pressure.

We would like to point out that the concept of a metamagnetic QCEP should be distinguished from a quantum critical point (QCP) that separates two phases with different symmetry. The QCEP is the endpoint of a line of first-order transitions that is tuned to zero temperature and as such it is an isolated singular point in the phase diagram that is surrounded by a single thermodynamic phase. In contrast, a QCP separates different thermodynamic phases, for example, a paramagnet and an antiferromagnet. The latter is actually realized in the Ge-doped sister compound CeRu₂(Si_{1-x}Ge_x)₂ close to concentrations $x \approx 0.06–0.07$.²⁵

For the comparison presented here, we performed new measurements on a single crystal of CeRu₂Si₂ grown by Czochralski method.²⁶ Thermal expansion, magnetostriction and heat-capacity measurements were carried out in a ³He/⁴He dilution refrigerator mounted inside an 18 T superconducting magnet. A capacitive dilatometer²⁷ made of CuBe and with high sensitivity of $\frac{\Delta L}{L_0} = 10^{-10}$ was used to estimate

the thermal-expansion coefficient $\alpha_c(H, T) = \frac{1}{L_{c0}} \frac{\partial L_c}{\partial T}$ and the magnetostriction coefficient $\lambda_c(H, T) = \frac{1}{L_{c0}\mu_0} \frac{\partial L_c}{\partial H}$ for $L \parallel c$. It is well known that in CeRu₂Si₂ the length change of the sample ΔL shows the same temperature and field dependence along all crystallographic axes but ΔL_c is three times larger than ΔL_a .¹⁴ For this reason, we scaled our data by a factor of $\frac{5}{3}$ to get the volume expansion α and magnetostriction λ . The heat capacity was measured by a silver platform using compensated heat-pulse technique.²⁸ In both experiments we tuned the magnetic field very close to the metamagnetic critical field H_m in ultrafine field steps of just a few mT. We were able to extend the temperature range of our measurements down to 60 mK in comparison to former publications. Our results reproduce nicely existing data for the same temperatures and fields of α , λ ,^{8,14–16} and the specific heat.^{11,29,30}

The paper is organized as follows. In Sec. II we discuss qualitatively the characteristic thermodynamics expected close to a metamagnetic QCEP, in Sec. III we discuss the metamagnetic signatures and their relationship in CeRu₂Si₂, and we end with a summary in Sec. IV.

II. UNIVERSAL SIGNATURES CLOSE TO A METAMAGNETIC QCEP

Close to a metamagnetic quantum critical endpoint the free energy density, $\mathcal{F} = \mathcal{F}_0 + \mathcal{F}_{\text{cr}}$, can be separated into a background part, \mathcal{F}_0 , and a critical part, \mathcal{F}_{cr} , deriving from the Ising QCEP

$$\mathcal{F}_{\text{cr}} = \mathcal{F}_{\text{cr}}(h, T, r). \quad (1)$$

We assume that \mathcal{F}_0 yields only a small, featureless background contribution to thermodynamics that is subleading compared to the critical one. The critical part in Eq. (1) depends on temperature, T , on the magnetic scaling field h that is conjugate to the Ising order parameter, and a parameter, r , that measures the distance to quantum criticality. A negative value, $r < 0$, corresponds to a finite endpoint temperature $T_{\text{ep}} > 0$, and for $r > 0$ only a metamagnetic crossover occurs. The QCEP is realized exactly for $r = 0$. Additionally, it is important how the magnetic scaling field, h , is related to the physical fields. Usually for endpoints, this relation is not evident as, e.g., for the liquid-gas transition, and, as a consequence, the Ising symmetry is often hidden. However, in our case the situation is more fortunate as we are dealing with an endpoint at $T = 0$. In the limit of a vanishing endpoint temperature $T_{\text{ep}} \rightarrow 0$, the line of first-order metamagnetic transitions will align itself with the temperature axis in the (H, T) phase diagram. This follows from the Clausius-Clapeyron relation after taking into account that the transition at $T = 0$ is between two ground states of same entropy, see Fig. 1. This alignment has the consequence that the magnetic scaling field, h , of the Ising QCEP can be directly identified with the distance to the critical magnetic field

$$h|_{T=0} = H - H_m. \quad (2)$$

The magnetic scaling field, h , thus controls the distance to the QCEP directly on the magnetic field axis and, as a result, the Ising symmetry becomes explicit in the (H, T) phase dia-

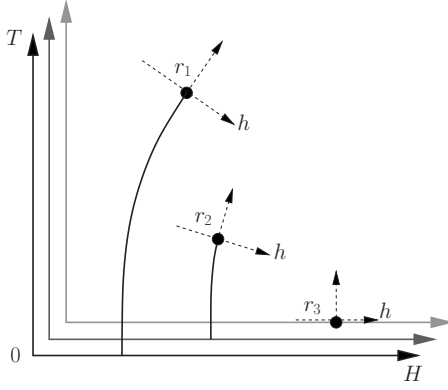


FIG. 1. Schematic depiction of planes in the H - T phase diagram with a critical endpoint, which terminates a line of a metamagnetic first-order transition. The parameter r is a measure of the distance to the QCEP in parameter space and three different cases r_1 , $r_1 < 0$, $r_1 < r_2 < 0$, and $r_3 = 0$ are shown. For $r > 0$ the endpoint disappears below the $T = 0$ axis, which corresponds to the situation in CeRu_2Si_2 . The dashed local coordinate system close to the endpoint aligns itself with the physical coordinates as the endpoint temperature approaches zero, $T_{\text{ep}} \rightarrow 0$.

gram. At a finite temperature, there will be a superlinear T correction to h even for the QCEP, $r = 0$; we will later see that for CeRu_2Si_2 this correction is of order $\mathcal{O}(T^2)$.

Within certain models,^{2,4,31} the critical free energy in Eq. (1) can be calculated and the dependences on its parameters can be determined. In the present work, we will follow a different route and concentrate on the generic properties that all these models for a metamagnetic QCEP have in common. We will therefore focus on a qualitative discussion of the universal metamagnetic signatures that derive from two basic assumptions: (i) a diverging differential susceptibility χ at the QCEP and (ii) its Ising universality.

Probably the most fundamental quantity, that characterizes the metamagnetic behavior, is the differential susceptibility χ

$$\chi = - \frac{\partial^2 \mathcal{F}}{\partial H^2}. \quad (3)$$

At a QCEP, $r = 0$, the susceptibility diverges upon decreasing temperature, T , or decreasing h

$$\chi|_{\text{QCEP}} \rightarrow \infty \text{ as } T, |h| \rightarrow 0. \quad (4)$$

This serves as our definition of quantum critical metamagnetism. We show below that this increase in χ close to the QCEP is responsible for all of the striking metamagnetic phenomena. The pronounced increase in the susceptibility χ in CeRu_2Si_2 at H_m only saturates at a temperature $T^* = 0.5$ K. In the QCEP scenario, this saturation temperature T^* is a measure of a finite positive parameter r in Eq. (1), $\lim_{T, |h| \rightarrow 0} \chi \sim 1/r$.

Apart from χ , we will discuss various other second-order derivatives of the free energy: the specific-heat coefficient γ , thermal expansion α , magnetostriction λ , and compressibility κ , defined as

$$\gamma = - \frac{\partial^2 \mathcal{F}}{\partial T^2}, \quad \alpha = \frac{\partial^2 \mathcal{F}}{\partial T \partial p}, \quad \lambda = \frac{\partial^2 \mathcal{F}}{\partial H \partial p}, \quad \kappa = - \frac{\partial^2 \mathcal{F}}{\partial p^2}. \quad (5)$$

The pressure dependence of the critical part \mathcal{F}_{cr} enters via the smooth pressure dependence of h , i.e., the critical field, $H_m = H_m(p)$. In the language of field theory, the pressure dependence of the other parameter r is less relevant and will be neglected in the following. It is convenient to define

$$\Omega_m = \frac{\partial H_m}{\partial p}. \quad (6)$$

For the small pressures applied in dilatometric experiments Ω_m can be approximated to be constant, $\Omega_m \approx \text{const}$.

Because of the scaling form in Eq. (1), the critical contributions to thermodynamic quantities are not independent. It follows from Eq. (1) that the critical part of the thermal expansion parallels the T derivative of the magnetization

$$\alpha_{\text{cr}} = \Omega_m \frac{\partial M_{\text{cr}}}{\partial T}, \quad (7)$$

where $M_{\text{cr}} = -\partial \mathcal{F}_{\text{cr}} / \partial H$. In addition, the critical parts of the susceptibility, magnetostriction, and compressibility are expected to be proportional

$$\chi_{\text{cr}} = \frac{1}{\Omega_m} \lambda_{\text{cr}} = \frac{1}{\Omega_m^2} \kappa_{\text{cr}}. \quad (8)$$

Such proportionalities have been observed in CeRu_2Si_2 (Refs. 15 and 32) and also in $\text{Sr}_3\text{Ru}_2\text{O}_7$.²² For a QCEP the susceptibility diverges by definition in Eq. (4), which in turn implies a divergence in the compressibility κ . This means that the crystal lattice is destabilized by strong metamagnetic fluctuations, and, as a consequence, the QCEP is likely to be preempted by a structural transition.^{33,34} We interpret the enormous crystal softening of up to 50% observed^{7,32} in CeRu_2Si_2 as a precursor of such a structural instability driven by metamagnetic fluctuations.

A strong increase in $\chi_{\text{cr}}(T)$ with decreasing T , Eq. (4), also has implications for the H dependence of the specific-heat coefficient, $\gamma_{\text{cr}}(H)$. Using the higher-order Maxwell relation

$$\frac{\partial^2 \gamma_{\text{cr}}}{\partial H^2} = \frac{\partial^2 \chi_{\text{cr}}}{\partial T^2} \quad (9)$$

it directly follows from a positive curvature of $\chi_{\text{cr}}(T)$ that $\gamma_{\text{cr}}(H)$ exhibits a characteristic minimum at H_m . This implies that the function $\gamma_{\text{cr}}(H)$ must first increase with increasing distance from H_m . It is clear that this increase in $\gamma_{\text{cr}}(H)$ cannot continue indefinitely so that the minimum at the critical field H_m is likely to be framed by two side peaks at finite h . Such a characteristic double-peak structure is observed in CeRu_2Si_2 (Ref. 11) and, for thermodynamic consistency, we predict it to occur in $\text{Sr}_3\text{Ru}_2\text{O}_7$ as well.³⁵ The saturation of χ in CeRu_2Si_2 at a temperature T^* is, according to Eq. (9), accompanied by a crossover from a minimum to a maximum in $\gamma(H)$ close to H_m in agreement with experimental observations.¹¹ In addition, from the side peaks of the specific-heat coefficient $\gamma_{\text{cr}}(H)$ we can infer with the help of the relation

$$\frac{\partial \gamma_{\text{cr}}}{\partial H} = \frac{\partial^2 M_{\text{cr}}}{\partial T^2} = \frac{1}{\Omega_m} \frac{\partial \alpha_{\text{cr}}}{\partial T} \quad (10)$$

a peak in the temperature dependence of the thermal expansion $\alpha_{\text{cr}}(T)$ at the same finite h .

Finally, we can exploit the Ising symmetry of the QCEP that demands that the free energy is an even function of the scaling field h

$$\mathcal{F}_{\text{cr}}(h, T, r) = \mathcal{F}_{\text{cr}}(-h, T, r). \quad (11)$$

This Ising symmetry implies, in particular, a sign change of the thermal expansion, $\alpha_{\text{cr}}(h) = -\alpha_{\text{cr}}(-h)$, at $h=0$. The position of the sign change in α is a good indicator for the strength of the subleading temperature dependence of the magnetic scaling field $h(T)$. If this temperature dependence can be neglected, the sign change of α is located exactly at $H=H_m$ and the Ising symmetry is explicit in the phase diagram. A finite-temperature dependence will shift the sign change away from H_m . Above, we argued that this T dependence will be superlinear due to the Clausius-Clapeyron relation. Characteristic sign changes in $\alpha(H)$ and peaks in $\alpha(T)$, see Eq. (10), have been observed in the metamagnetic materials CeRu_2Si_2 ,⁹ $\text{Sr}_3\text{Ru}_2\text{O}_7$,³⁶ and $\text{Ca}_{1.8}\text{Sr}_{0.2}\text{RuO}_4$.³⁷ It has been shown³⁸ that such sign changes of the thermal expansion are generic for quantum criticality and reflect the accumulation of entropy.

In the presence of a QCEP, $r=0$, it follows from general arguments³⁹ that the Grüneisen parameter defined as the ratio of thermal expansion and specific heat, $\Gamma_{\text{cr}} = \alpha_{\text{cr}}/(\gamma_{\text{cr}}T)$, saturates in the low-temperature limit to a value given by

$$\Gamma_{\text{cr}}|_{\text{QCEP}} \xrightarrow{T \rightarrow 0} \Omega_m \frac{G}{H - H_m}, \quad (12)$$

where the prefactor G is a combination of critical exponents.³⁹ The sign change in Γ at H_m reflects again the one mentioned above in the thermal expansion. Note that if the QCEP is only approximately realized, $r>0$, as in CeRu_2Si_2 the divergence Eq. (12), will be cutoff sufficiently close to H_m and the sign change of Γ will not go through infinity but through zero instead.³³ The quantum critical enhancement of Γ , Eq. (12), offers a convenient explanation for the anomalous large values of the Grüneisen parameter observed in CeRu_2Si_2 .^{6,8}

At some finite distance to the QCEP, the critical free energy in Eq. (1) will be an analytic function of h in the limit $h \rightarrow 0$, and the limiting behavior

$$\mathcal{F}_{\text{cr}}|_{T>0} \approx f_{\text{cr}}(T) - \frac{1}{2} \chi_{\text{max}}(T) h^2 + \mathcal{O}(h^4) \quad (13)$$

is expected. For positive $r>0$, this expansion should also apply at $T=0$. Note that the expansion starts quadratically in h due to the Ising symmetry in Eq. (11). The next-order correction of order $\mathcal{O}(h^4)$ is positive so that $\chi_{\text{max}}(T)$ corresponds to the maximum value of $\chi_{\text{cr}}(h)$ at fixed temperature T , see Eq. (4). Expression (13) implies some interesting relations between thermodynamic quantities. The susceptibility for vanishing scaling field h , $\chi_{\text{max}}(T) = \chi_{\text{cr}}(h=0, T)$, does not only determine the curvature of $\gamma_{\text{cr}}(H)$ close to H_m , see Eq.

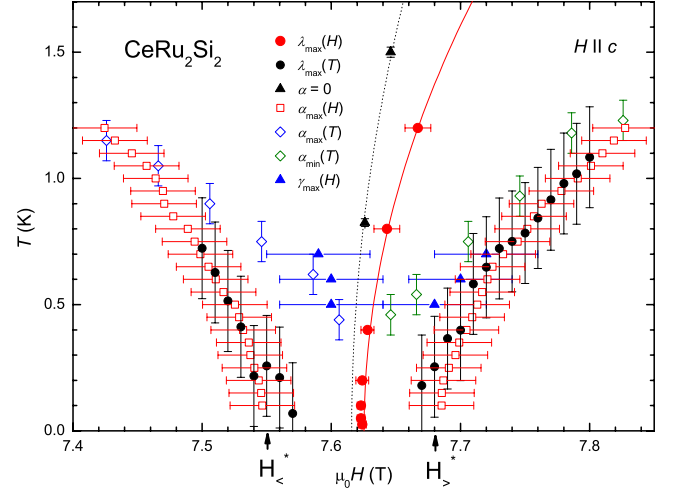


FIG. 2. (Color online) Magnetic field-temperature (H, T) plane of CeRu_2Si_2 close to its metamagnetic field $\mu_0 H_m = 7.62$ T with the positions of extrema in magnetostriction, $\lambda(H)$ and $\lambda(T)$, thermal expansion, $\alpha(H)$ and $\alpha(T)$, specific heat $\gamma(H)$, and the positions of vanishing thermal expansion. Note that the drift of the positions of maxima in $\lambda(H)$, away from H_m spoils the explicit Ising symmetry. Critical divergencies in thermodynamics are cutoff upon entering the pocket enclosed by the positions of extrema in $\alpha(H)$ and $\alpha(T)$ close to H_m ; its extension can be quantified by the temperature and field scale, $T^* = 0.5$ K and $h^* = (H_*^+ - H_*^-)/2 = 0.07$ T/ μ_0 , respectively, which are measures of the distance to the QCEP in parameter space, see text.

(9), but also defines the limiting form of the thermal expansion

$$\alpha_{\text{cr}}|_{T>0} \approx \Omega_m \chi'_{\text{max}}(T) h + \mathcal{O}(h^3), \quad (14)$$

where $\chi'_{\text{max}} = \partial_T \chi_{\text{max}}$. The thermal expansion is expected to depend linearly on $h \approx H - H_m$ with a prefactor given by the derivative of the critical differential susceptibility. Note, however, that we neglect in Eq. (14) contributions from the superlinear temperature dependence of the magnetic scaling field $h(T)$.

III. COMPARISON WITH CeRu_2Si_2

In the following, we discuss in more detail the signatures in thermal expansion, magnetostriction, and specific heat of CeRu_2Si_2 close to the metamagnetic field H_m . The phase diagram close to H_m in Fig. 2 summarizes the positions of maxima and minima in magnetostriction, $\lambda(T)$ and $\lambda(H)$, thermal expansion, $\alpha(T)$ and $\alpha(H)$, and specific heat, $\gamma(H)$ and also shows where the thermal expansion becomes zero. For $T \rightarrow 0$, the positions of the maxima in magnetostriction $\lambda(H)$ approach and, thus, identify the critical field $\mu_0 H_m \approx 7.62$ T. At finite temperatures, the positions of these maxima and, similarly, the positions of vanishing thermal expansion deviate from H_m by a distance proportional to T^2 , shown by the solid and dotted line, respectively. We interpret this deviation as arising from a T dependence of the magnetic scaling field $h(T)$ that spoils the explicit Ising symmetry in the phase diagram.

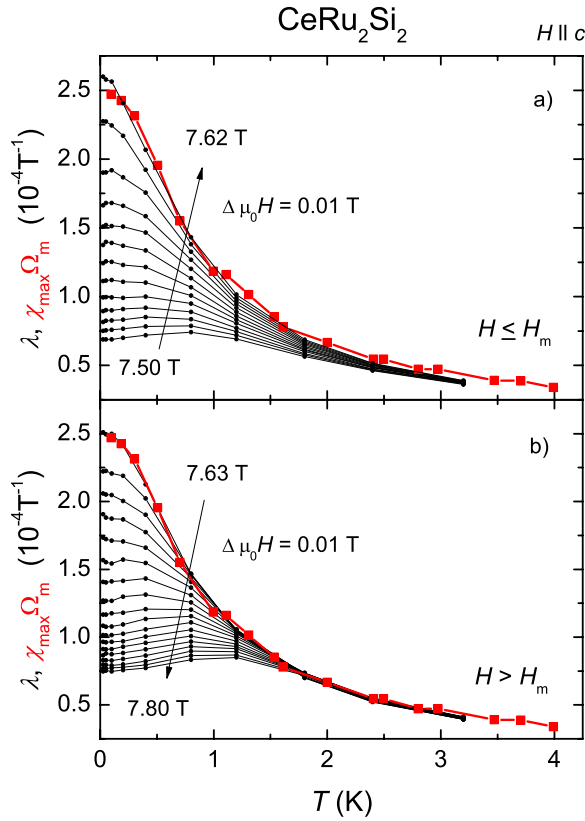


FIG. 3. (Color online) Magnetostriction $\lambda(T)$ for different magnetic fields close to $\mu_0 H_m = 7.62$ T; panels (a) and (b) show $\lambda(T)$ for fields $H \leq H_m$ and $H > H_m$, respectively, in steps of 0.01 T. For comparison, T dependence of maxima $\chi_{\max}(T)$ in the differential susceptibility $\chi(H)$ from Ref. 7 are shown (red squares) identifying a proportionality factor $\Omega_m = 1.5 \pm 0.1$ T kbar $^{-1}$, see Eq. (8).

A. Magnetostriction

Magnetostriction as a function of field, $\lambda(H)$, has been already presented in Refs. 8 and 15. In Fig. 3, we focus, alternatively, on the temperature dependence of our magnetostriction data for different fields close to H_m . Upon decreasing temperature, $\lambda(T)$ first increases. Away from the critical field, $\lambda(T)$ reaches a maximum and then decreases again until it saturates at a constant value in the limit $T \rightarrow 0$. For fields close to H_m , this maximum however disappears and $\lambda(T)$ increases monotonously with decreasing T . The magnetostriction close to the critical field has the largest absolute values identified by the envelope, $\lambda_{\max}(T)$, of the set of $\lambda(T)$ curves in Fig. 3. In the following arguments, the proportionality of magnetostriction and differential susceptibility χ will be of importance; this correspondence was impressively demonstrated in Ref. 15. Here, we show this correspondence again by comparing the envelope of $\lambda(T)$ curves with the temperature dependence of the maxima in $\chi(H)$ data taken from Ref. 7 (red squares in Fig. 3). The proportionality factor determines Ω_m as defined in Eq. (6). We obtain the value $\Omega_m = 1.5 \pm 0.1$ T kbar $^{-1}$, which is slightly smaller than the value of 2.0 T kbar $^{-1}$ estimated by pressure experiments.⁴⁰ The magnetostriction at the critical field saturates below the characteristic temperature $T^* = 0.5$ K, which

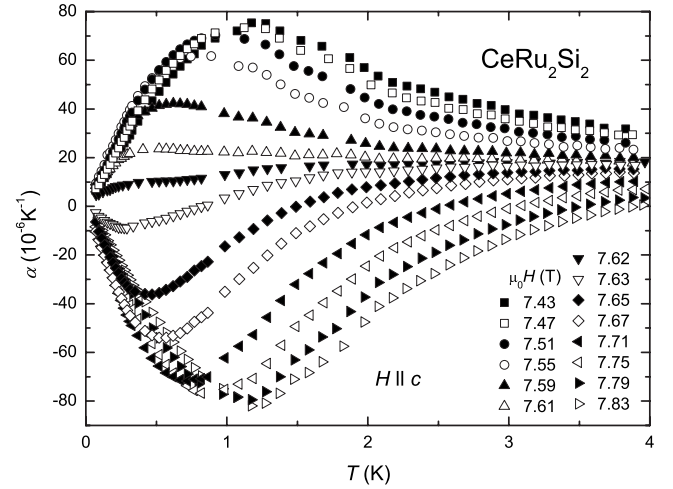


FIG. 4. Thermal expansion as a function of temperature for various magnetic fields close to $\mu_0 H_m = 7.62$ T. The curves are approximately mirror symmetric due to the emergent Ising symmetry of the QCEP.

we identify as a crossover from critical to noncritical behavior associated with a finite distance to the QCEP in parameter space. As we will see below, the inflection point of $\lambda(T)$ located at T^* will also determine crossover signatures in other thermodynamic quantities.

The positions of the characteristic maxima in $\lambda(T)$ are shown in the (H, T) plane of Fig. 2. Interestingly, the maxima in $\lambda(T)$ and $\chi(T)$ imply, according to the relation

$$\frac{\partial \lambda_{\text{cr}}}{\partial T} = \Omega_m \frac{\partial \chi_{\text{cr}}}{\partial T} = \frac{\partial \alpha_{\text{cr}}}{\partial H} \quad (15)$$

an extremum in the field dependence of the thermal expansion, $\alpha_{\text{cr}}(H)$, at the same positions in the phase diagram, which we will confirm below. Note that characteristic maxima in the temperature dependence of $\chi(T)$, which are, according to Eq. (8), equivalent to the maxima in $\lambda(T)$ of Fig. 3, have been also observed in the metamagnetic material $\text{Sr}_3\text{Ru}_2\text{O}_7$.⁴¹

B. Thermal expansion

Thermal-expansion data of CeRu_2Si_2 has been presented in Refs. 9 and 14. Already in zero field, $H=0$, $\alpha(T)$ exhibits a peak that shifts to lower temperatures and sharpens with increasing H . At the critical field H_m , thermal expansion changes sign, and the negative peak in $\alpha(T)$ broadens and shifts to higher temperatures for increasing fields $H > H_m$. This behavior is reminiscent of quantum critical metamagnetism as discussed in some detail in Ref. 36. Similar behavior of $\alpha(T)$ is observed near the metamagnetic field of $\text{Sr}_3\text{Ru}_2\text{O}_7$ (Ref. 36) and $\text{Ca}_{1.8}\text{Sr}_{0.2}\text{RuO}_4$.³⁷ A closer inspection, however, reveals that the behavior very close to the critical field differs qualitatively from the theoretical expectations for a QCEP, see Fig. 4. When the peak position has reached a temperature on the order of $T^* = 0.5$ K, it does not shift further toward lower temperatures upon increasing H , but its height instead decreases to zero and reemerges with

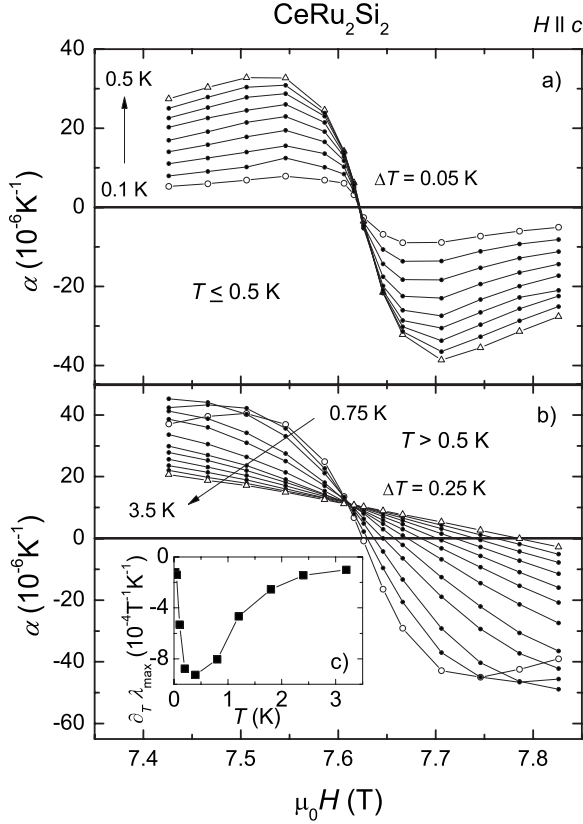


FIG. 5. Thermal expansion as a function of field H for various temperatures obtained by extrapolation from the data set in Fig. 4. Panels (a) and (b) show temperatures $T \leq T^*$ and $T > T^*$, respectively, with $T^* = 0.5$ K and steps $\Delta T = 0.05$ K and $\Delta T = 0.25$ K, respectively. Their slope close to the critical field is given by $\partial_H \alpha|_{H=H_m} \approx \partial_T \lambda_{\max}$ whose T dependence is shown in the inset (c). Its extremal value for the slope, $\min\{\partial_T \lambda_{\max}\} \approx -0.001$ (T K) $^{-1}$, at T^* determines the bundling slope of the $\alpha(H)$ curves close to H_m in panel (a).

opposite sign for fields $H > H_m$. The thermal expansion curve $\alpha(T)$ then almost recovers its shape but with opposite sign. We interpret this qualitative change as a crossover from critical to noncritical behavior associated with the temperature scale T^* . For temperatures $T < T^*$, the thermal expansion has temperature dependence $\alpha \propto T$ characteristic for a Fermi liquid.

The dense data set in Fig. 4 allows to discuss the magnetic field dependence of the thermal expansion at a given temperature, $\alpha(H)$. The extrapolated curves are shown in Figs. 5(a) and 5(b) for temperatures $T \leq T^*$ and $T > T^*$, respectively. For low temperatures, $T \leq T^*$, $\alpha(H)$ has a point reflection symmetry located at $H = H_m$ and $\alpha = 0$ which is characteristic for an emergent Ising symmetry close to a critical endpoint. The absolute value of thermal expansion $|\alpha(H)|$ first increases upon approaching the critical field H_m but after reaching an extremum it decreases and vanishes at H_m . The positions of these extrema in $\alpha(H)$ are shown in Fig. 2. As argued above, these positions in the phase diagram coincide with the positions of corresponding maxima in $\lambda(T)$. In the low-temperature limit they extrapolate to the fields $\mu_0 H_{<}^* = 7.55$ T and $\mu_0 H_{>}^* = 7.68$ T; their distance identifies a finite

field scale $h^* = (H_{>}^* - H_{<}^*)/2 = 0.07$ T μ_0^{-1} attributed to the vanishing of the extrema in $\lambda(T)$ and $\alpha(H)$. This finite field scale $\mu_0 h^* = 0.07$ T indicates that the increase in $|\alpha(H)|$ while approaching H_m always gives way to a decrease even at lowest temperatures. Hence, it signifies a crossover from critical to noncritical behavior at $T = 0$ and is thus a magnetic field analog of the temperature scale T^* .

Furthermore, note that the curves $\alpha(H)$ in Fig. 5(a) tend to bundle near H_m to a line with constant slope. Generally, the slope of $\alpha(H)$ can be identified with the derivative of magnetostriction $\partial_T \lambda$ or, equivalently, of the susceptibility $\partial_T \chi$. The numerical derivative of $\lambda_{\max}(T)$, the envelope in Fig. 3, is shown in Fig. 5(c). It is its minimum value, $\min\{\partial_T \lambda_{\max}\} = -0.001$ (T K) $^{-1}$, at T^* that identifies the bundling slope in Fig. 5. Moreover, the two lines in the phase diagram that identify the extrema of $\alpha(H)$ are also the boundaries of the region where the analytic expansion of the critical free energy in the scaling field in Eq. (13) holds. Well within this region the thermal expansion depends linearly on $H - H_m$ as expected from Eq. (14).

For larger temperatures, $T > T^*$, the thermal expansion $\alpha(H)$ is shown in Fig. 5(b). Apparently, the field range where $\alpha(H)$ is approximately linear increases, see Eq. (14), its slope decaying with increasing temperature in accordance with the behavior of $\partial_T \lambda_{\max}$. In contrast to the low-temperature limit, the curves do not intersect at $H = H_m$ and $\alpha = 0$ anymore, which we attribute to the incipient T dependence of the magnetic scaling field h that breaks the explicit Ising symmetry.

C. Specific heat

Specific-heat data have been reported in Ref. 11. The specific-heat coefficient γ is enhanced close to the critical field by almost a factor of 2 compared to its zero-field value. However, one observes a sharp single peak close to H_m only at lowest temperatures, $T < T^*$. At elevated temperatures, $T > T^*$, a double-peak structure in $\gamma(H)$ with a minimum at H_m is found. In the following, we focus on the behavior of γ close to the critical field (see inset of Fig. 6) and, in particular, analyze the minimum/maximum crossover at T^* . The fitted curvatures of $\gamma(H)$ at the extremum close to H_m are shown in Fig. 6 for each available temperature. The result is compared to the numerical second-order derivative of $\lambda_{\max}(T)$ or, equivalently, $\chi_{\max}(T)$ of Fig. 3. As anticipated from Eq. (9), the two quantities agree within the error bars. In particular, the minimum/maximum crossover is identified with the *inflection point* of $\chi_{\max}(T)$ at $T \approx T^*$ where $\partial_T^2 \chi_{\max}(T) = 0$. In the phase diagram Fig. 2, we also show the positions of the side peaks in $\gamma(H)$ (not shown in Fig. 6) that coincide within the error bars with the positions of the maxima in $\alpha(T)$ as expected from Eq. (10).

IV. SUMMARY

We presented a comprehensive discussion of the universal thermodynamic signatures, which emerge close to a metamagnetic quantum critical endpoint. We argued that (i) the diverging differential susceptibility together with (ii) the Ising symmetry of the QCEP account for the following char-

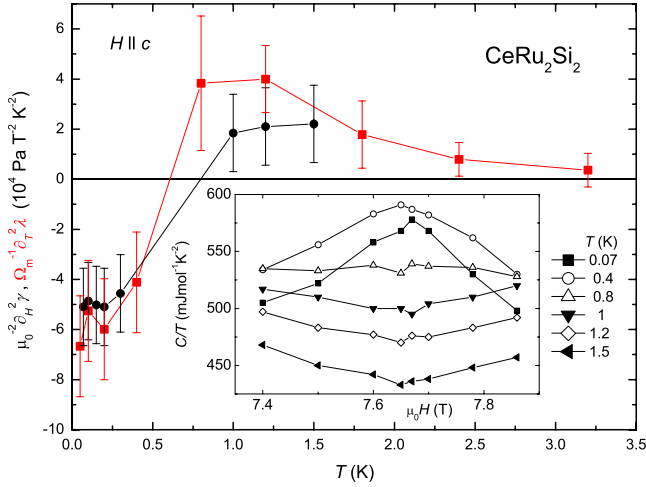


FIG. 6. (Color online) The specific-heat coefficient $\gamma(H)$ exhibits a minimum/maximum crossover close to the critical field H_m with decreasing temperature, see inset. The main panel shows the curvature $\partial_H^2 \gamma(H)$ (black circles) at the extremum close to H_m as a function of T , which is compared to $\partial_T^2 \lambda_{\max} / \Omega_m$ (red squares). By virtue of Eq. (9), the minimum/maximum crossover of $\gamma(H)$ is determined by an inflection point in the susceptibility, $\partial_T^2 \chi_{\max} = \partial_T^2 \lambda_{\max} \Omega_m^{-1} = 0$, at $T^* = 0.5$ K.

acteristics of critical metamagnetism: (1) a proportionality between susceptibility, magnetostriction, and compressibility in the presence of a magnetoelastic coupling and, as a result, (2) a pronounced crystal softening, (3) an enhanced Grüneisen parameter, (4) a sign change of the thermal expansion at the critical field, and (5) a minimum in the specific-heat coefficient $\gamma(H)$. The latter minimum directly follows from the Maxwell relation $\partial_T^2 \chi = \partial_H^2 \gamma$ and the positive curvature of the susceptibility. A minimum in $\gamma(H)$, in turn, implies two side peaks, and we showed that their positions in the (H, T) plane coincide with the extrema in the thermal expansion $\alpha(T)$ as a function of temperature. The Ising symmetry of the endpoint ensures that the sign change of the thermal expansion $\alpha(H)$ due to entropy accumulation³⁸ occurs close to the critical field H_m .

As an example, we discussed the metamagnetic compound CeRu_2Si_2 , which shows pronounced metamagnetic signatures that saturate, however, at very low temperatures, $T^* = 0.5$ K, and close to the critical field, $|H - H_m| < h^*$

$= 0.07 \text{ T} \mu_0^{-1}$. We argued that outside this regime in the phase-diagram behavior for a metamagnetic QCEP is expected. We presented high-precision data close to the critical field, that allowed us, in particular, to analyze the crossover from critical to noncritical behavior associated with the temperature and field scale, T^* and h^* , respectively. We demonstrated that the onset of saturation in the differential susceptibility $\chi(T)|_{H=H_m}$ at T^* leads to an inflection point that accounts for the minimum-to-maximum crossover in the specific-heat coefficient $\gamma(H)$ at H_m . Furthermore, we demonstrated that the derivative $\partial_T \chi(T)|_{H=H_m}$ determines the temperature dependence of the thermal expansion close to the critical field. The inflection point at T^* is reflected by an extremum in $\alpha(T)$ at the same temperature as the critical field is approached. We also demonstrated that the magnetostriction $\lambda(T)$ and, equivalently, the differential susceptibility $\chi(T)$ has a maximum as a function of temperature only for fields $|H - H_m| > h^*$ allowing us to identify the field scale $\mu_0 h^* = 0.07$ T. Such characteristic maxima have been observed also in the metamagnetic compound $\text{Sr}_3\text{Ru}_2\text{O}_7$.⁴¹ We pointed out that these maxima coincide with thermodynamically equivalent extrema in the thermal expansion $\alpha(H)$.

The focus of the present work are the qualitative thermodynamic signatures close to quantum critical metamagnetism, irrespective of the microscopic details of the material and the precise model describing the critical dynamics of the order-parameter fluctuations. We checked, however, that all signatures discussed here for CeRu_2Si_2 are reproduced qualitatively within the QCEP model introduced in Ref. 4, which will be the subject of a separate publication.

The universal metamagnetic signatures have been here illustrated on the heavy-fermion compound CeRu_2Si_2 . We hope that this work will motivate further experimental investigations to identify additional materials that are close to a metamagnetic QCEP.

ACKNOWLEDGMENTS

We acknowledge P. Haen for providing the high-quality single crystal and J. A. Mydosh for fruitful discussions about CeRu_2Si_2 . Discussion with T. Lorentz on metamagnetism in $\text{Ca}_{1.8}\text{Sr}_{0.2}\text{RuO}_4$ is gratefully acknowledged as well. The work was funded by the DFG under Grants No. FOR 960 and No. SFB 608 (M.G.) and by the Max-Planck Society under Project M.FE.A.CHPHSM (F.W.).

¹E. P. Wohlfarth and P. Rhodes, *Philos. Mag.* **7**, 1817 (1962).

²H. Yamada, *Phys. Rev. B* **47**, 11211 (1993).

³S. A. Grigera, R. S. Perry, A. J. Schofield, M. Chiao, S. R. Julian, G. G. Lonzarich, S. I. Ikeda, Y. Maeno, A. J. Millis, and A. P. Mackenzie, *Science* **294**, 329 (2001).

⁴A. J. Millis, A. J. Schofield, G. G. Lonzarich, and S. A. Grigera, *Phys. Rev. Lett.* **88**, 217204 (2002).

⁵P. Haen, J. Flouquet, F. Lapiere, P. Lejay, and G. Remenyi, *J. Low Temp. Phys.* **67**, 391 (1987).

⁶J. Flouquet, in *Heavy Fermion Matter*, Prog. Low Temp. Phys,

edited by W. Halperin (Elsevier, Amsterdam, 2005), Vol. XV.

⁷J. Flouquet, S. Kambe, L. P. Regnault, P. Haen, J. P. Brison, F. Lapiere, and P. Lejay, *Physica B* **215**, 77 (1995).

⁸A. Lacerda, A. de Visser, P. Haen, P. Lejay, and J. Flouquet, *Phys. Rev. B* **40**, 8759 (1989).

⁹A. Lacerda, A. de Visser, L. Puech, P. Lejay, P. Haen, J. Flouquet, J. Voiron, and F. J. Okhawa, *Phys. Rev. B* **40**, 11429(R) (1989).

¹⁰I. Kouroudis, D. Weber, M. Yoshizawa, B. Luthi, L. Puech, P. Haen, J. Flouquet, G. Bruls, U. Welp, J. J. M. Franse, A. Men-

- ovsky, E. Bucher, and J. Hufnagl, *Phys. Rev. Lett.* **58**, 820 (1987).
- ¹¹Y. Aoki, T. D. Matsuda, H. Sugawara, H. Sato, H. Ohkuni, R. Settai, Y. Onuki, E. Yamamoto, Y. Haga, A. V. Andreev, V. Sechovsky, L. Havela, H. Ikeda, and K. Miyake, *J. Magn. Magn. Mater.* **177**, 271 (1998).
- ¹²S. Holtmeier, P. Haen, A. Lacerda, P. Lejay, J. L. Tholence, J. Voiron, and J. Flouquet, *Physica B* **204**, 250 (1995).
- ¹³T. Sakakibara, T. Tayama, K. Matsuhira, H. Mitamura, H. Amitsuka, K. Maezawa, and Y. Onuki, *Phys. Rev. B* **51**, 12030(R) (1995).
- ¹⁴C. Paulsen, A. Lacerda, L. Puech, P. Haen, P. Lejay, J. L. Tholence, J. Flouquet, and A. de Visser, *J. Low Temp. Phys.* **81**, 317 (1990).
- ¹⁵K. Matsuhira, T. Sakakibara, A. Nomachi, T. Tayama, K. Tenya, H. Amitsuka, K. Maezawa, and Y. Onuki, *J. Phys. Soc. Jpn.* **68**, 3402 (1999).
- ¹⁶K. Matsuhira, T. Sakakibara, K. Maezawa, and Y. Onuki, *J. Phys. Soc. Jpn.* **68**, 2420 (1999).
- ¹⁷F. J. Ohkawa, *Solid State Commun.* **71**, 907 (1989).
- ¹⁸D. M. Edwards and A. C. M. Green, *Z. Phys. B* **103**, 243 (1997).
- ¹⁹H. Satoh and F. J. Ohkawa, *Phys. Rev. B* **63**, 184401 (2001).
- ²⁰D. Meyer and W. Nolting, *Phys. Rev. B* **64**, 052402 (2001).
- ²¹J. Flouquet, P. Haen, S. Raymond, D. Aoki, and G. Knebel, *Physica B* **319**, 251 (2002).
- ²²S. A. Grigera, P. Gegenwart, R. A. Borzi, F. Weickert, A. J. Schofield, R. S. Perry, T. Tayama, T. Sakakibara, Y. Maeno, A. G. Green, and A. P. Mackenzie, *Science* **306**, 1154 (2004).
- ²³J.-M. Mignot, J. Flouquet, P. Haen, F. Lapiere, L. Puech, and J. Voiron, *J. Magn. Magn. Mater.* **76-77**, 97 (1988).
- ²⁴F. Weickert, P. Gegenwart, J. A. Mydosh, F. Steglich, C. Kanadani, Y. Tabata, T. Taniguchi, and S. Kawarazaki, *Physica B* **359**, 68 (2005).
- ²⁵P. Haen, H. Bioud, and T. Fukuhara, *Physica B* **259**, 85 (1999).
- ²⁶P. Haen, CRTBT, CNRS Grenoble, 38042 Grenoble, France.
- ²⁷R. Pott and R. Schefzyk, *J. Phys. E* **16**, 444 (1983).
- ²⁸H. Wilhelm, T. Luehmann, T. Rus, and F. Steglich, *Rev. Sci. Instrum.* **75**, 2700 (2004).
- ²⁹R. A. Fisher, N. E. Phillips, C. Marcenat, J. Flouquet, P. Haen, P. Lejay, and J.-M. Mignot, *J. Phys.* **49**, C8 (1988).
- ³⁰K. Heuser, E.-W. Scheidt, T. Schreiner, Z. Fisk, and G. R. Stewart, *J. Low Temp. Phys.* **118**, 235 (2000).
- ³¹B. Binz and M. Sigrist, *Europhys. Lett.* **65**, 816 (2004).
- ³²G. Bruls, D. Weber, B. Lüthi, J. Flouquet, and P. Lejay, *Phys. Rev. B* **42**, 4329 (1990).
- ³³M. Garst (unpublished).
- ³⁴A. P. Levanyuk and A. A. Sobyenin, *Sov. Phys. JETP* **11**, 371 (1970).
- ³⁵A. W. Rost, R. S. Perry, J.-F. Mercure, A. P. Mackenzie, and S. A. Grigera, *Science* **325**, 1360 (2009).
- ³⁶P. Gegenwart, F. Weickert, M. Garst, R. S. Perry, and Y. Maeno, *Phys. Rev. Lett.* **96**, 136402 (2006).
- ³⁷J. Baier, P. Steffens, O. Schumann, M. Kriener, S. Stark, H. Hartmann, O. Friedt, A. Revcolevschi, P. G. Radaelli, S. Nakatsuji, Y. Maeno, J. A. Mydosh, T. Lorenz, and M. Braden, *J. Low Temp. Phys.* **147**, 405 (2007).
- ³⁸M. Garst and A. Rosch, *Phys. Rev. B* **72**, 205129 (2005).
- ³⁹L. Zhu, M. Garst, A. Rosch, and Q. Si, *Phys. Rev. Lett.* **91**, 066404 (2003).
- ⁴⁰H. Aoki, M. Takashita, M. Kimura, T. Terashima, S. Uji, T. Matsumoto, and Y. Onuki, *J. Phys. Soc. Jpn.* **70**, 774 (2001).
- ⁴¹S.-I. Ikeda, Y. Maeno, S. Nakatsuji, M. Kosaka, and Y. Uwatoko, *Phys. Rev. B* **62**, R6089 (2000).